

# The impact of the Three Gorges Dam on the fate of metal contaminants across the river–ocean continuum

Maodian Liu<sup>a,b,c</sup>, Yipeng He<sup>a,b</sup>, Zofia Baumann<sup>b,d</sup>, Qianru Zhang<sup>a,e</sup>, Xin Jing<sup>a,f</sup>, Robert P. Mason<sup>b</sup>, Han Xie<sup>a</sup>, Huizhong Shen<sup>g</sup>, Long Chen<sup>h</sup>, Wei Zhang<sup>i</sup>, Qianggong Zhang<sup>j</sup>, Xuejun Wang<sup>a,\*</sup>

<sup>a</sup> Ministry of Education Laboratory of Earth Surface Processes, College of Urban and Environmental Sciences, Peking University, Beijing 100871, China

<sup>b</sup> Department of Marine Sciences, University of Connecticut, 1080 Shennecossett Rd., Groton, CT 06340, United States

<sup>c</sup> School of the Environment, Yale University, New Haven, CT 06511, United States

<sup>d</sup> Billion Oyster Project, Governors Island, New York, NY 10004, United States

<sup>e</sup> School of Earth and Atmospheric Sciences, Georgia Institute of Technology, Atlanta, GA 30332, United States

<sup>f</sup> Rubenstein School of Environment and Natural Resources, University of Vermont, Burlington, Vermont 05405, United States

<sup>g</sup> School of Civil and Environmental Engineering, Georgia Institute of Technology, Atlanta, GA 30332, United States

<sup>h</sup> Key Laboratory of Geographic Information Science (Ministry of Education), East China Normal University, Shanghai 200241, China

<sup>i</sup> School of Environment and Natural Resources, Renmin University of China, Beijing 100872, China

<sup>j</sup> Key Laboratory of Tibetan Environment Changes and Land Surface Processes, Institute of Tibetan Plateau Research, Chinese Academy of Sciences, Beijing 100101, China

## ARTICLE INFO

### Article history:

Received 14 February 2020

Revised 26 July 2020

Accepted 12 August 2020

Available online 13 August 2020

### Keywords:

River damming

River–ocean continuum

Downstream hydrological impact

Contaminant accumulation and

resuspension

Soil erosion

## ABSTRACT

The Three Gorges Dam (TGD) is the world's largest hydropower construction. It can significantly impact contaminant transport in the Yangtze River–East China Sea Continuum (YR–ECSC). In addition to evaluating the impact of the TGD on the deposition of contaminants in the reservoir, we also address their cycles in the river below the dam and in the coastal East China Sea. A comprehensive study of metal contaminant transport along the YR–ECSC has not been previously attempted. We quantified the fates of mercury (Hg), arsenic (As), lead (Pb), cadmium (Cd) and chromium (Cr) within the YR–ECSC, and the impacts of the TGD, by sampling water and suspended particles along the Yangtze River during spring, summer, fall, and winter and by modeling. We found that the Yangtze River transports substantial amounts of heavy metals into the coastal ocean. In 2016, riverine transport amounted to 48, 5900, 11,000, 230, and 15,000 megagrams (Mg) for Hg, As, Pb, Cd, and Cr, respectively, while other terrestrial contributions were negligible. Metal flux into the coastal ocean was primarily derived from the downstream portion of the river (84–97%), while metals transported from upstream were largely trapped in the Three Gorges Reservoir (TGR, 72%–96%). For example, 34 Mg of Hg accumulated in the TGR owing to river damming, large-scale soil erosion, and anthropogenic point source releases, while 21 Mg of Hg was depleted from the riverbed downstream owing to the altered river hydrology caused by the TGD. Overall the construction of TGD resulted in a 6.9% net decrease in the Hg burden of the East China Sea, compared to the pre-TGD period.

© 2020 Elsevier Ltd. All rights reserved.

## 1. Introduction

The pollution of the environment with heavy metals poses severe threats to wildlife and human health when these metals are bioavailable and assimilate into the food web (Cheng, 2003; Volesky and Holan, 1995). Among the diverse range of heavy metal contaminants that enter the aquatic environment, mercury

(Hg), arsenic (As), lead (Pb), cadmium (Cd) and chromium (Cr) are the most toxic to organisms, and are therefore the most studied by environmental researchers (Durube et al., 2007; Järup, 2003; Nriagu and Pacyna, 1988). The cycling of heavy metals in the environment has been the subject of various studies, primarily focusing on the atmosphere (Nriagu, 1989; Pacyna et al., 2006; Pirrone et al., 2010; Streets et al., 2011; Wai et al., 2016). However, rivers can serve as the primary delivery routes of these heavy metals, as well as other contaminants, to the coastal ocean (Amos et al., 2014; Matschullat, 2000; Schartup et al., 2015). According to previous research, 54–61 Gg/yr of As and 0.3–5.5 Gg/yr

\* Corresponding author.

E-mail address: [xjwang@urban.pku.edu.cn](mailto:xjwang@urban.pku.edu.cn) (X. Wang).

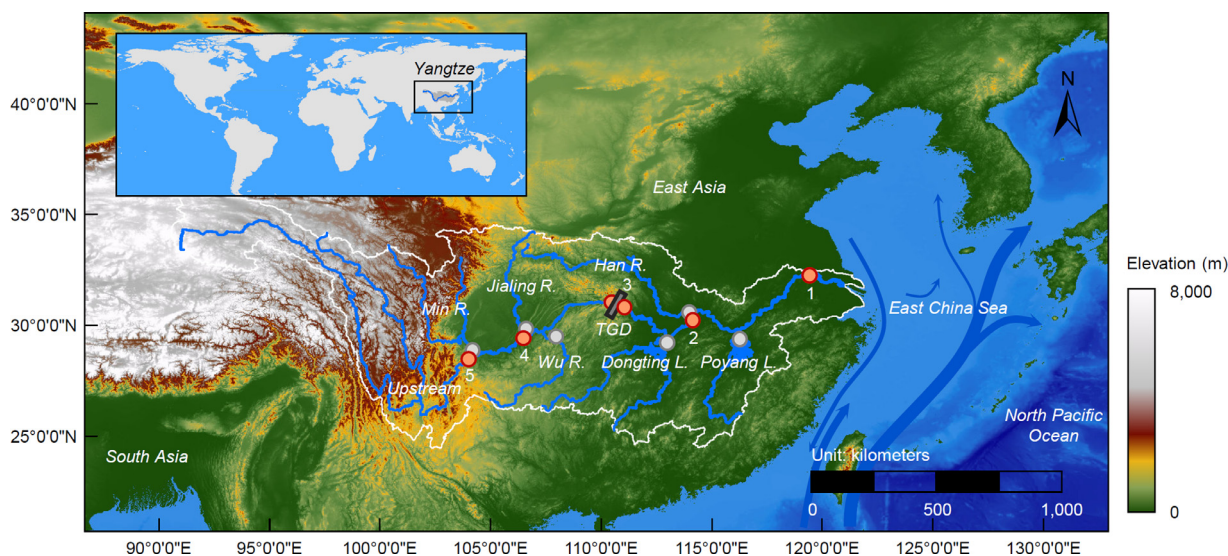


**Fig. 1.** Location of sampling sites across the Yangtze River Basin. Orange and gray dots represent sampling sites in the main stream and major tributaries of the river basin, respectively. R, River; L, Lake; 1, Nanjing; 2, Wuhan; 3, Yichang; 4, Chongqing; and 5, Yibin.

of Hg are exported by rivers to the global ocean (Amos et al., 2014; Matschullat, 2000; Outridge et al., 2018) but the contributions of individual rivers remain unknown. The impact of regional-scale variation in river hydrology, owing to anthropogenic or natural environmental change, has been shown to dramatically impact metal transport, as well as the biogeochemical processes in the associated terrestrial and ocean environments, both regionally and globally, and this impact is of global significance (Poff et al., 2007; Regnier et al., 2013; Syvitski et al., 2005). Specifically, the construction and operation of hydroelectric dams can significantly alter element transport (Humborg et al., 1997; Ittekkot et al., 2000; Maavara et al., 2017). Globally, river damming has induced substantial amounts of phosphorous (P) and organic carbon (C) accumulation in reservoirs (Maavara et al., 2017; Maavara et al., 2015), but the impact of damming on toxic heavy metal transport is not well understood. Upon their entry into riverine ecosystems, highly particle-reactive elements, such as Hg, Pb, Cd, Cr, and (less so) As, are scavenged by suspended particles and transported downstream toward the sea in the particulate phase. Therefore, any obstruction to river flow, such as that caused by dams, might substantially impact the transport of these elements, and must be considered when evaluating metal inventories and fluxes, and when assessing environmental risks in both freshwater and their linked marine ecosystems.

Worldwide, there are ~50,000 dams that are defined as “large,” based on height (i.e.,  $\geq 15$  m) or reservoir capacity (i.e.,  $> 3$  km<sup>3</sup>) (Lempérière, 2006). The Three Gorges Dam (TGD, Fig. S1, Supporting Information, SI), situated halfway along the Yangtze River, provides a dramatic example of the impact of large reservoirs. It is the largest dam (i.e., 185 m high  $\times$  2,335 m long) in the world in terms of the amount of hydroelectricity that it can generate (Stone, 2008; Wu et al., 2003). The Yangtze River, supports a human population of 500 million, is known both for having a large geographic span, and being one of the most developed industrial areas in the world (Fig. 1). As the third longest river in the world, it is also classified as the fourth largest in its delivery of both riverine water and suspended sediment into the sea (Dai et al., 2008; Yang et al., 2002). A rapid shift in upstream sediment deposition and downstream elevated sediment transport dynamics has occurred in the Yangtze River owing to the construction of the TGD (Müller et al., 2008; Wu et al., 2003; Yang et al., 2014). Before the construction of the TGD (1956–2002), the upper portion of the Yangtze River, which

we define as upstream of the TGD, yielded 490 Tg/yr of sediment to the lower portion, while sedimentation in the lower portion occurred at a rate of 78 Tg/yr (Yang et al., 2014). In contrast, during the post-TGD decade, the annual deposition of suspended sediment in the Three Gorges Reservoir (TGR) was 190 Tg, while the water released from the TGR annually eroded 63 Tg of sediment from the river downstream (Yang et al., 2014). While selected studies have focused on heavy metal contamination in the TGR (Gao et al., 2019; Zhu et al., 2019), the impacts of the reservoir on levels in the Yangtze River–East China Sea Continuum (YR–ECSC) post-TGD construction have thus far received little attention. The lack of knowledge of the impact of sediment trapping by the TGR and downstream erosion during the post-construction period on heavy metal transport, motivated the present study.

Therefore, in this study we aimed to evaluate the impact of the TGD on fluxes of Hg, As, Pb, Cd, and Cr, in their particulate and dissolved phases, from the Yangtze River into the East China Sea. Our study combined field observations and diverse modeling approaches. To obtain estimates of heavy metal concentrations, including their partitioning between the dissolved and particulate phases, we collected water samples from different locations in the Yangtze River Basin (Fig. 1), covering 3,300 km of the river across four seasons in 2016. The water samples were filtered to separate the particulate and dissolved phases. We then modeled the fate of heavy metals in the YR–ECSC during the period from 1990–2016 by integrating long-term observations of metal concentrations and freshwater and suspended sediment discharges before and after the construction of the TGD, using previously generated data (Table S1, SI). The overall aim of this study is to elucidate the magnitude of the impact of a large dam on the cycling and transport of toxic metal contaminants in a large river–ocean continuum, and to provide support for the assessment of health risks to people who rely on seafood harvested from impacted Asian coastlines.

## 2. Materials and Methods

### 2.1. Sample collection

To calculate the transport of heavy metals in the Yangtze River, we collected samples from different sites that were located near gauging stations in the main stream, and from the major tributaries along the river (Fig. 1). We sampled during four seasons

in 2016 using previously published techniques (Buck et al., 2015; Liu et al., 2019b). For the main stream of the river (Fig. 1), samples were collected in four different seasons. For the major tributaries, which were characterized by the largest amounts of freshwater or sediment discharges into the main stream of the river (MWR, 2016b), samples were collected during the dry (Oct and Jan) and wet (Jun and July) seasons (Liu et al., 2019b). Detailed information about the sampling sites is provided in our previous study (Liu et al., 2019b). The influence of the tide at our sampling sites in the river mouth was assumed to be negligible as freshwater flux dominates in those areas (Liu et al., 2019b). At each sampling site, 1,000 mL of water was sampled in triplicate or quadruplicate from the central portion of the river. During each season, the sampling of the sites in the Yangtze River mouth occurred over a period of 3–4 consecutive days.

During sampling, diverse boats were utilized, based on available opportunities, and high-speed trains or long-distance buses were employed to travel to the sampling sites. Water sampling was conducted only on days with no precipitation (Liu et al., 2017). As described in our previous study, river water was sampled from 1 m below the surface into acid-cleaned amber-glass bottles (Liu et al., 2019b). To avoid contamination during sampling, we used the “clean hands / dirty hands” technique (Emmert et al., 2013; Liu et al., 2019b). To collect the suspended sediment, a volume ranging from 300–1,000 mL of bulk water was filtered in triplicate or quadruplicate through a 0.45- $\mu\text{m}$  pore size cellulose nitrate membrane (Whatman, product code 10401170). The filtrate was preserved via acidification by adding 4 mL (equal to a volume-based concentration of 0.4%) of 11.6 M trace-metal-grade HCl in the field. The preserved water samples and filters were stored in incubators under cool, dark conditions, and delivered to the lab within 24 h. Prior to analysis, the preserved, filtered water samples were stored at 4°C and in dark conditions, while the filters were kept at -20°C and then dried at approximately 60°C to determine their particulate mass, prior to digestion and analysis (Liu et al., 2019b).

## 2.2. Analytical methodology

The analyses for dissolved total Hg (referred throughout the rest of the manuscript as dissolved Hg) were made in duplicate, following U.S. EPA method 1631E. Briefly, to determine the dissolved Hg, we added BrCl to all samples to oxidize the organic matter and all forms of Hg. Next, we added  $\text{NH}_2\text{OH}\cdot\text{HCl}$  to the digested samples to degrade any remaining free halogens. Finally, to convert Hg(II) into Hg(0), we added  $\text{SnCl}_2$  and vigorously shook each sealed vial before analysis. All samples for dissolved Hg were analyzed at the *Institute of Tibetan Plateau Research* using a cold vapor atomic fluorescence spectrometer (Tekran model 2600). To gain particulate Hg concentration data, the filters were analyzed in duplicate using a direct mercury analyzer, the DMA80 (U.S. EPA method 7473), at *Peking University* (Hammerschmidt et al., 2006). The detection limits for the dissolved and particulate Hg analyses were 0.1 ng/L and 0.05 ng/g, respectively. The recoveries for the dissolved and particulate Hg analyses were  $92 \pm 7\%$  and  $97 \pm 5\%$ , respectively.

The analyses of the other metals, i.e., As, Pb, Cd, and Cr, were conducted using an inductively coupled plasma mass spectrometer at the *Institute of Geographic Sciences and Natural Resources Research*. We digested the filters with their suspended sediment samples, using an  $\text{HNO}_3/\text{HClO}_4/\text{HF}$  mixture, in Teflon vessels in a graphite oven at approximately 140°C overnight, as previously described (Liu et al., 2018a). We dried and dissolved the digestion solutions using dilute 5% vol./vol.  $\text{HNO}_3$ . Both the dissolved and particulate samples for these four metals were measured in duplicate. The detection limits were 0.08, 0.003, 0.003, and 0.07  $\mu\text{g/L}$  for As, Pb, Cd, and Cr, respectively, and the recoveries for the above metals were  $96 \pm 3\%$ ,  $85 \pm 17\%$ ,  $95 \pm 10\%$ , and  $94 \pm 7\%$ , respec-

tively. The data on the dissolved organic C (DOC) concentrations in the same water samples, were taken from a previously published dataset (Liu et al., 2019b).

## 2.3. Heavy metal transport in the Yangtze River

To characterize the transport patterns of the five elements, including their dissolved and particulate phases, in the Yangtze River, a previously published modeling framework that considers the source–sink processes of each contaminant was adopted (Liu et al., 2019b). Probabilistic distributions for the concentrations of heavy metals were computed by Monte Carlo simulation. Fluxes of heavy metals at the main stream and major tributary sampling sites were calculated as shown below:

$$F(x, y) = \sum_i (C(x)_i \times M_i \times K_i) + \sum_j (C(y)_j \times V_j \times K_j) \quad (1)$$

where  $F(x, y)$  is the probabilistic distribution of the transport flux of each heavy metal in each sampling site (unit: Gg/yr),  $C(x)$  is the probabilistic distribution of the dissolved concentration of each heavy metal ( $\mu\text{g/L}$ ),  $C(y)$  is the probabilistic distributions of the particulate concentration of each heavy metal ( $\mu\text{g/g}$ ),  $V$  is the annual transport volume of riverine water or wastewater ( $\text{km}^3/\text{yr}$ ),  $M$  is the annual transport mass of suspended sediment (Tg/yr), and  $K$  is the unit conversion factor. Other heavy metal export pathways from land to sea were acknowledged in our calculations (description to follow). Hence,  $i$  represents different dissolved-phase discharge pathways, and  $j$  represents different particulate-phase discharge fractions.

In our previous study, we estimated the extent of the lateral transport of heavy metals induced by soil erosion in China (Liu et al., 2019c). However, quantification of the discharge of select metals (i.e., As, Pb, Cd, and Cr) from anthropogenic point sources into the waters of the Yangtze River is lacking. This lack of knowledge makes it difficult to quantify the impacts of the TGD on this transport during the post-TGD period. To gain insight into the impact made by the TGD on metal transport across the river, we focus on Hg in this study. Therefore, we quantify both the impact of the TGD and those of external sources, including soil erosion and industrial and municipal wastewater discharges (Liu et al., 2019c; Liu et al., 2018b; Liu et al., 2016b). The method of source apportionment in the Yangtze River was discussed in detail in our previous study (Liu et al., 2019b). Briefly, the analysis was begun by estimating the Hg discharges from the major tributaries and external sources to the main stream, followed by evaluating Hg transport in the main stream. In the final step, Hg export into the coastal East China Sea or net accumulation in the riverbed was assessed (Liu et al., 2019b). Consistent with our previous study, we did not consider the contribution of the direct deposition of atmospheric Hg, as this source is negligible (Liu et al., 2019b).

## 2.4. Heavy metal transport from land to sea

We constructed an inventory of present-day heavy metal (Hg, As, Pb, Cd, and Cr) export from mainland China to the East China Sea, including inputs from rivers, wastewater, groundwater, soil erosion, and coastal erosion (in all five pathways, heavy metals are discharged into the coastal ocean directly), as reported in a previous study (Liu et al., 2016a). The calculation method for these five pathways is the same as described by eq. (1). The heavy metal concentrations in riverine water were obtained from published literature and our measurements (Table S1, SI). The heavy metal concentrations in wastewater were obtained from Zhao et al. (Zhao et al., 2014). The heavy metal concentrations in groundwater and coastal soils are provided in Table S2 and Table S3 in the SI. The coastal

soil erosion rates and moduli were also updated in this study and are provided in Tables S4 and S5.

To obtain heavy metal concentration variations at the Yangtze River mouth, a one-dimensional, normal distribution function was applied to estimate the variation following a previous study, as indicated below (Streets et al., 2011):

$$y_{m,t} = \left( \frac{a_m \pm SE}{(\sigma_m \pm SE) \pm \sqrt{2\pi}} \right) \times e^{-\left(\frac{t-p_m}{\sigma_m \pm SE}\right)^2} + (b_m \pm SE) \quad (2)$$

where  $y$  represents the concentration of the heavy metal,  $a$  is a constant term representing the highest point of the fitted normal distribution,  $\sigma$  is the shape parameter of the curve,  $\pi$  is the ratio of the circumference of a circle to its diameter,  $t$  represents the time series (depending on the time scale of the measurement data of each heavy metal),  $p$  is the time of peak concentration based on the measurement data,  $b$  represents the baseline of the fitted normal distribution,  $m$  represents each heavy metal, and  $SE$  is the standard error of each parameter. This normal curve has been previously applied to simulate the dynamics of pollution change in terms of pollution emission factors (Streets et al., 2011) and energy and emission control technology (Grübler et al., 1999), and can be used to estimate both the historical and future release trends of pollution at any point in time (Bond et al., 2007; Streets et al., 2004). The parameter values for each heavy metal are provided below:

$$y_{Hg,t} = \left( \frac{1000 \pm 350}{(4.1 \pm 1.4) \pm \sqrt{2\pi}} \right) \times e^{-\left(\frac{t-2010}{4.1 \pm 1.4}\right)^2} + (72 \pm 21),$$

$$R^2 = 0.78 \quad (3)$$

$$y_{As,t} = \left( \frac{15 \pm 5.7}{(2.7 \pm 1.1) \pm \sqrt{2\pi}} \right) \times e^{-\left(\frac{t-2006}{2.7 \pm 1.1}\right)^2} + (4.6 \pm 0.39),$$

$$R^2 = 0.68 \quad (4)$$

$$y_{Pb,t} = \left( \frac{180 \pm 99}{(5.0 \pm 2.7) \pm \sqrt{2\pi}} \right) \times e^{-\left(\frac{t-2002}{5.0 \pm 2.7}\right)^2} + (13 \pm 3.4),$$

$$R^2 = 0.56 \quad (5)$$

$$y_{Cd,t} = \left( \frac{3.7 \pm 2.2}{(7.5 \pm 4.1) \pm \sqrt{2\pi}} \right) \times e^{-\left(\frac{t-2005}{7.5 \pm 4.1}\right)^2} + (0.20 \pm 0.066),$$

$$R^2 = 0.32 \quad (6)$$

$$y_{Cr,t} = \left( \frac{1600 \pm 410}{(14 \pm 3.5) \pm \sqrt{2\pi}} \right) \times e^{-\left(\frac{t-1988}{14 \pm 3.5}\right)^2} + (10 \pm 7.3),$$

$$R^2 = 0.88 \quad (7)$$

all the SE values of each equation were considered in the uncertainty analysis.

### 2.5. Mass balance model

To gain insight into the impacts of the TGD on the fate of heavy metals in the coastal ocean, we developed marine mass balances for the five heavy metals of interest (Liu et al., 2016a). The major source terms in this mass balance model included the river, wastewater, groundwater, soil erosion, coastal erosion, ocean currents, and dry and wet deposition, while the major sinks included sedimentation of settling particles, gas evasion into the atmosphere, bioaccumulation in fish and fishing, and oceanward transport via ocean currents. The parameters of the model are provided in Table S6, SI. Seven major rivers (Fig. S2, SI) flowing into the East China Sea, i.e., the Yangtze River, Min River, Qiantang River, Jiu-long River, Huangpu River, Jin River, and Huotong River, were included in the inventory of the estimated riverine heavy metal con-

tributions to the sea. The freshwater discharge from these seven major rivers accounts for more than 95% of all the contributions of rivers to the sea (MWR, 2016b). If a data source provided only dissolved- or particulate-phase information, eq. (8) was applied to calculate the other concentration, as described in a previous study (Amos et al., 2014):

$$\log_{10}K_D = \log_{10}\left(\frac{C_p \times 1000}{C_D}\right) \quad (8)$$

where  $\log_{10}K_D$  is the log-transformed partition coefficient,  $C_p$  is the concentration of the particulate metal ( $\mu\text{g/g}$ ), and  $C_D$  is that of the dissolved phase ( $\mu\text{g/L}$ ).

To evaluate the long-term impact of the TGD on heavy metal fluxes to the East China Sea, we divided the 1990–2016 data series of annual discharge from the Yangtze River into pre- (before 2003) and post-TGD (after 2003) periods. Additionally, the modeling considered two scenarios for the post-TGD period. The first scenario tested for the influence of the TGD on heavy metal discharge from the Yangtze River following 2003, while the second scenario assumed that the TGD was never constructed (no-TGD), to gain further insight into the impact of the TGD. To gain initial insight into the magnitude of heavy metal discharge for the no-TGD scenario, we assumed that heavy metal concentrations at the mouth of the Yangtze River (marine end-member) would be similar in both these scenarios, given limited biogeochemical data for the period prior to TGD construction. We excluded any influence of DOC in our simulations owing to the absence of any significant relationships between DOC and the concentrations of these heavy metals in our measurements. This assumption is consistent with a previous study, which argued that DOC was not suitable for the estimation of the riverine Hg transport in industrialized or contaminated basins, where perturbation by anthropogenic Hg input was independent of DOC (Amos et al., 2014). Furthermore, the suspended sediment loads discharged from the Yangtze River into the East China Sea in the no-TGD scenario were estimated based on the sediment transport estimates of Yang et al. (Yang et al., 2014).

### 2.6. Structural equation model

The structural equation model (SEM) framework is a modeling technique that can be used as an effective analytical tool to explore the relationships between variables and to test different direct and indirect causal hypotheses (Fig. S3, SI) (Mayor et al., 2017). We applied a piecewise SEM to examine the direction and magnitude of four explanatory variables on the heavy metal discharges from the Yangtze River into the East China Sea: precipitation, surface temperature, water impoundment by the TGD, and the gross domestic product (GDP) of the Yangtze River Basin. Annual precipitation and surface temperatures were used to represent regional climate conditions. Water impoundment, known to strongly decrease the transport of sediment (sediment flux) to the sea (Yang et al., 2014), was used as a proxy for the impact of the TGD. Riverine metal fluxes are also influenced by anthropogenic point source releases into inland waters. However, long-term inventories of the point source releases of these metals are not available. Given that the quantities of wastewater released are mainly driven by economic development in developing countries (Chen et al., 2016; Raschid-Sally and Jayakody, 2009), we used GDP as a proxy for the impacts of human activities on metal fluxes. To examine the robustness of the SEM, we used Shipley's test of *directed separation*, Fisher's C statistic and the AIC value to test the goodness-of-fit of the SEM (Shipley, 2013). We reported the standardized coefficient for each path (all the variables are scaled by mean and variance) and the marginal  $R^2$  for each component of the SEM (Lefcheck, 2016). All statistical analyses were conducted using R version 3.3.3.

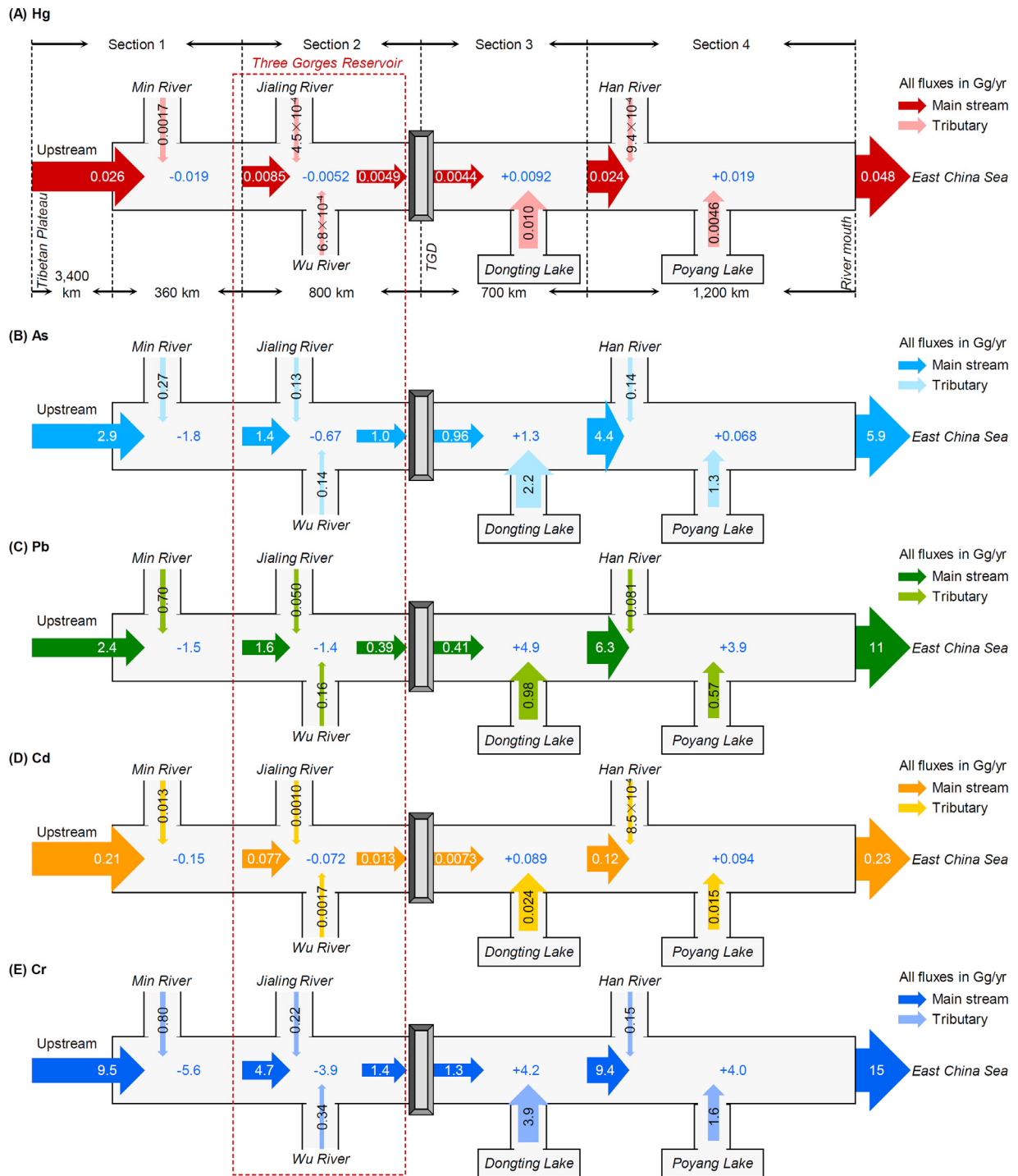


**Fig. 2.** Heavy metal transport in the Yangtze River Basin in 2016. Panels (A) to (E) represent Hg, As, Pb, Cd, and Cr, respectively. For illustrative purposes, we use log transformations to draw the arrows.

### 2.7. Uncertainty analysis

A Monte Carlo simulation (10,000 runs) was applied to analyze the robustness of all the inventories and material flows of the five marine mass balance models. The concentrations of heavy metals are assumed to follow log-normal distributions based on previously published measurements (An et al., 2010; Lin et al., 2000). We calculated the median values and P10–90 confidence intervals of the statistical distributions of the heavy metal fluxes or concentrations to represent the uncertainty of the individual heavy metal

fluxes. Furthermore, we compared the results with observational data from previous studies to ensure the rationality of the model results. For the SEM modeling results, we report the standard errors of the standardized coefficients in Fig. S4, SI.

### 2.8. Data availability

The freshwater and suspended sediment discharge data for these rivers were derived from yearbooks (MWR, 2016b). The precipitation and surface temperature data were obtained from

the National Meteorological Information Center ([www.nmic.gov.cn](http://www.nmic.gov.cn)). The TGD water impoundment data were acquired from Yang et al. (2014). The GDPs of the provinces in the river basin were obtained from the China Statistical Yearbook (NBS, 2014). Data regarding inputs from external sources into the water column were taken from our previous studies (Liu et al., 2019c; Liu et al., 2018b; Liu et al., 2016b). The sources of the heavy metal concentrations and model parameters are provided in the SI.

### 3. Results and discussion

#### 3.1. Heavy metal discharge from the Yangtze River to the adjacent sea

In this study, we found that the Yangtze River could transport substantial amounts of heavy metals into the coastal ocean. In total, 32 Gg of heavy metals were discharged from the Yangtze River into the East China Sea in 2016. As for individual metals, 0.048 Gg of Hg, 5.9 Gg of As, 11 Gg of Pb, 0.23 Gg of Cd, and 15 Gg of Cr were discharged from the river into the sea (Fig. 2). The Yangtze River, therefore, serves as a significant source of heavy metal pollution for the East China Sea (Fig. S5, SI) and the global ocean (Table S7, SI). This is primarily driven by the massive transport of sediment and freshwater from the river into the sea (Syvitski et al., 2005; Yang et al., 2014).

Wet seasons, with their higher discharge, are responsible for a surprisingly large proportion of the annual heavy metal fluxes from the Yangtze River into the East China Sea. For example, 0.039 Gg of Hg, 4.3 Gg of As, 10 Gg of Pb, 0.20 Gg of Cd, and 14 Gg of Cr were discharged from the river into the coastal zone in the wet season in 2016, accounting for 82%, 73%, 94%, 85%, and 91% of their annual fluxes, respectively (Fig. 3). Previous studies have suggested that there is a significant positive relationship between contaminant concentration and riverine freshwater discharge (Lawson et al., 2001; Raymond et al., 2016; Sonke et al., 2018), similar to As, Cd, and Cr in the study area (Fig. 3). In contrast, the Hg and Pb concentrations in the Yangtze River mouth in spring were slightly higher than those of the other three seasons, which might be influenced by anthropogenic point source releases.

#### 3.2. Impacts of the TGD on heavy metal transport in the Yangtze River Basin

Based on the results of our modeling, we argue that heavy metal transport throughout the Yangtze River has been significantly altered by the TGD. Rivers that are not hydrologically altered (i.e., no dams) transport sediment eroded from the upstream areas to depositional areas downstream (Brandt, 2000), a transport pattern included in the “no-TGD” scenario in the Yangtze River (Yang et al., 2014). Moreover, in 2016, 15 Gg of heavy metals (0.026 Gg of Hg, 2.9 Gg of As, 2.4 Gg of Pb, 0.21 Gg of Cd, and 9.5 Gg of Cr) were transported from the upstream portion of the river to the TGR (Fig. 2), owing to severe soil erosion in the upstream regions of the Yangtze River Basin, as showed in our recent studies (Liu et al., 2019c; Liu et al., 2018b). A previous study by Yang et al. (2014) showed that up to 98% of the suspended particles that enter the reservoir can be removed from the water column via particle settling, owing to the reduced flow rate induced by the TGD (Yang et al., 2014). Accordingly, a large mass of the heavy metals that enter the TGR are subsequently deposited in the TGR. This deposition accounted for 72–96% of the total imports from rivers to the TGR in 2016. These values are similar to those of the deposition of suspended particles (i.e., 98%) that enter the reservoir. Subsequently, only a relatively small fraction of these metals is discharged into the downstream region from the reservoir, accounting for 3.2–16% of the river-related fluxes in

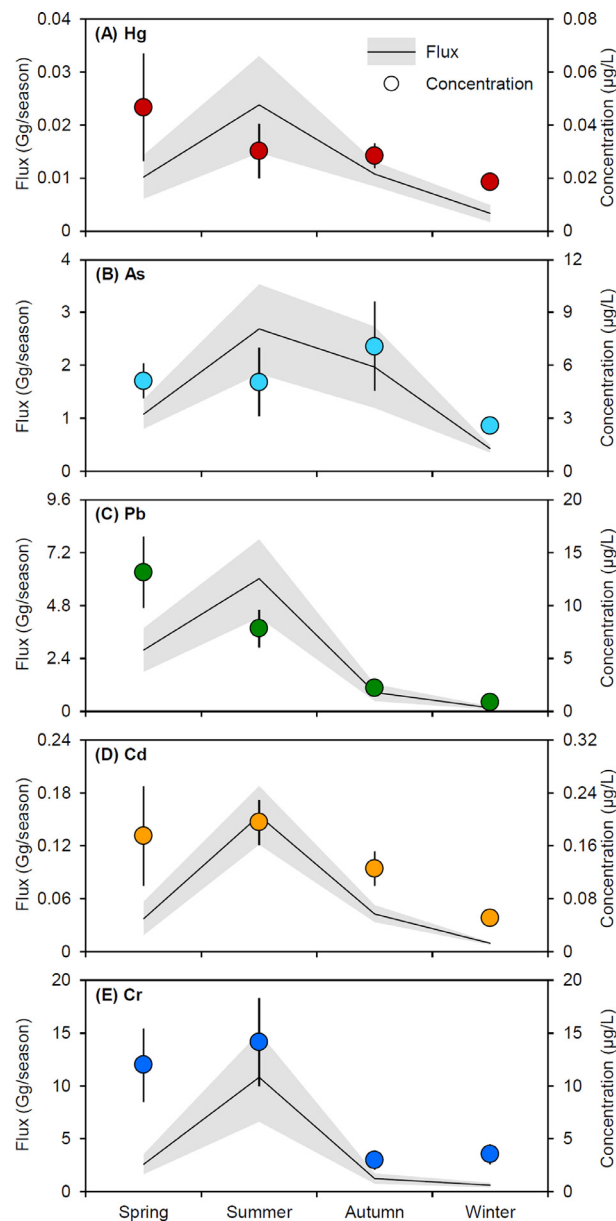


**Fig. 3.** Seasonal changes of heavy metal discharges from the Yangtze River into the East China Sea and their concentrations in the river mouth in 2016. Panels (A) to (E) represent Hg, As, Pb, Cd, and Cr, respectively. Shaded areas and error bars represent the standard deviations of the measurement.

the coastal ocean (Fig. 2). This pattern of diminished loads reaching the sea has been previously described for P and organic C (Maavara et al., 2017; Maavara et al., 2015).

Nevertheless, metal concentrations in the downstream portion of the Yangtze River increased, resulting in 0.029, 1.3, 8.9, 0.18, and 8.2 Gg fluxes for Hg, As, Pb, Cd, and Cr, respectively. These loads account for 61%, 22%, 81%, 80%, and 54% of their fluxes in the coastal ocean, respectively (Fig. 2), suggesting input from sources other than downstream tributaries. Moreover, with the exception of As ( $R = 0.27$ ,  $P = 0.11$ ,  $n = 41$ ), the significant positive relationships between total suspended sediment (TSS) and metal concentration (Hg:  $R = 0.68$ ,  $P < 0.01^{**}$ ; Pb:  $R = 0.75$ ,  $P < 0.01^{**}$ ; Cd:  $R = 0.69$ ,  $P < 0.01^{**}$ ; and Cr:  $R = 0.73$ ,  $P < 0.01^{**}$ , Table S8, SI) in the river water suggest that hydrological events, such as precipitation, dominate the dynamics of these heavy metals at a large, watershed scale (Fig. 3 and Fig. S6, SI). This is similar to the mech-

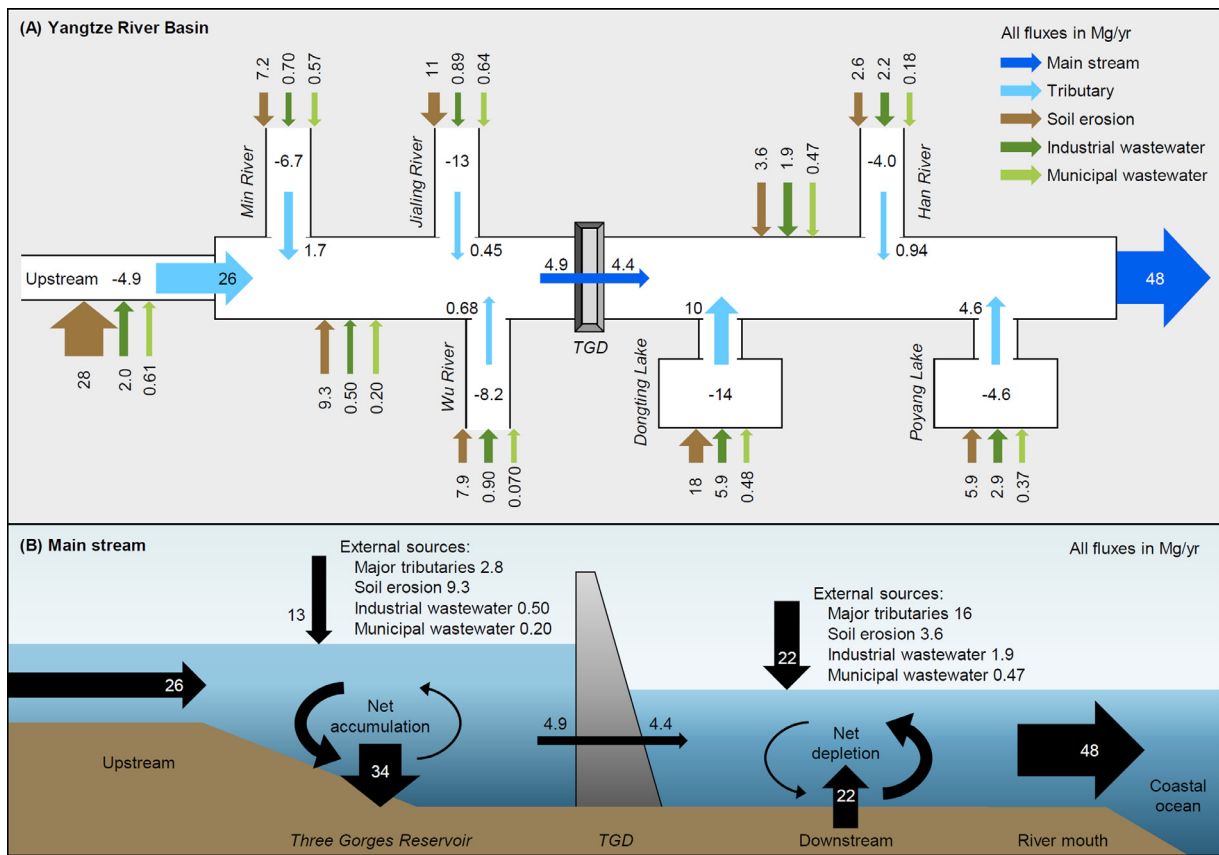


**Fig. 4.** Hg transport in the Yangtze River Basin. (A) is the external source of Hg in the river basin. (B) is the impact of the TGD on Hg transport. Data on Hg imports from external sources were obtained from the published literature (Liu et al., 2019c; Liu et al., 2018b; Liu et al., 2016b).

anism controlling organic matter transport (Raymond et al., 2016). According to Yang et al. (2014), the TSS concentrations in the water column increased 8-fold in the downstream section of the Yangtze River, and this is attributed mainly to the downstream hydrological impact of the TGD (which contributes 80% to the total imports), followed by flux from the six major tributaries (16%), and soil erosion (4%) (Yang et al., 2014). Based on the water samples that we collected from the central portion of the Yangtze River, downstream of the TGD, fluxes of Hg, Pb, Cd, and Cr were primarily bound by particulate matter (82%, 81%, 69%, and 83%, respectively), while As remained predominantly in the dissolved phase (65%). Therefore, the impact that the operation of the TGD has on hydrology and sediment erosion can significantly influence the metal fluxes in the East China Sea.

Further focusing on Hg, we quantified the impact of the TGD on Hg transport in the downstream portion of the Yangtze River. Based on the material flow analysis, soil erosion (120 Mg/yr including main stream and tributary basins) accounted for the majority of Hg in the entire Yangtze River Basin, followed by industrial (22 Mg/yr) and municipal wastewater (4.4 Mg/yr) (Fig. 4A). Soil erosion accounted for 92% and 72% of external Hg import in the upstream section of the river and the TGR (Fig. 4), respectively, and was attributed to intensive agriculture and the relatively steep slopes of the landforms in Southwest China (Liu et al., 2019c). In the downstream section of the Yangtze River, where soil erosion is less intense, the contribution of soil erosion to Hg was slightly smaller (17% of the total imports) than those in the upstream section of the river and the TGR (Liu et al., 2018b).

Based on our analyses, in 2016, 34 Mg of Hg accumulated in the TGR, and 22 Mg of Hg was depleted from the riverbed

downstream, owing to the altered hydrology caused by the TGD (Fig. 4B). Consequently, the flux of Hg from the TGD to the river mouth increased by a factor of 11, while the Hg concentration increased 3.4-fold. These increases are mainly attributed to TGD-induced downstream bank and riverbed erosion (22 Mg/yr), with additional inputs contributed by external sources (16, 3.6, and 2.4 Mg/yr by major tributaries, soil erosion, and point source releases, respectively; Fig. 4B). Previous studies have shown that water released from large reservoirs has a high transport capacity and relatively low TSS concentration, and is capable of enhancing riverbed erosion downstream of the dam (Brandt, 2000; Yang et al., 2014). This effect is also associated with the higher erodibility of the river bank and riverbed in this region, as verified by hydrological gauging stations in the Yangtze River (riverbed erosion rates of 0.1–1.4 m/yr in the downstream portion after the construction of the TGD) (MWR, 2016a). During the flood season, Hg and other metals already deposited in the reservoir might be re-suspended owing to high water discharge from the reservoir (Brandt, 2000; Vukovic et al., 2014). Based on our calculations, however, this phenomenon was not significant in the Yangtze River (Figs. 2 and 4).

Fluxes of As, Pb, Cd, and Cr, including their particulate and dissolved phases, in the main stream of the Yangtze River showed similar trends to Hg (Figs. 2 and 3), i.e., decreased upstream of the dam and general increasing downstream during their transport. This suggests that the TGD has similar impacts on them. Moreover, based on our measurements, the average water-particulate partition coefficient ( $\log K_D$ ) values for Pb and As were  $5.3 \pm 1.3$  and  $4.1 \pm 0.36$ , respectively, throughout the Yangtze River in 2016, showing that the level of Pb particle enrichment is an order of magnitude higher than that of As.

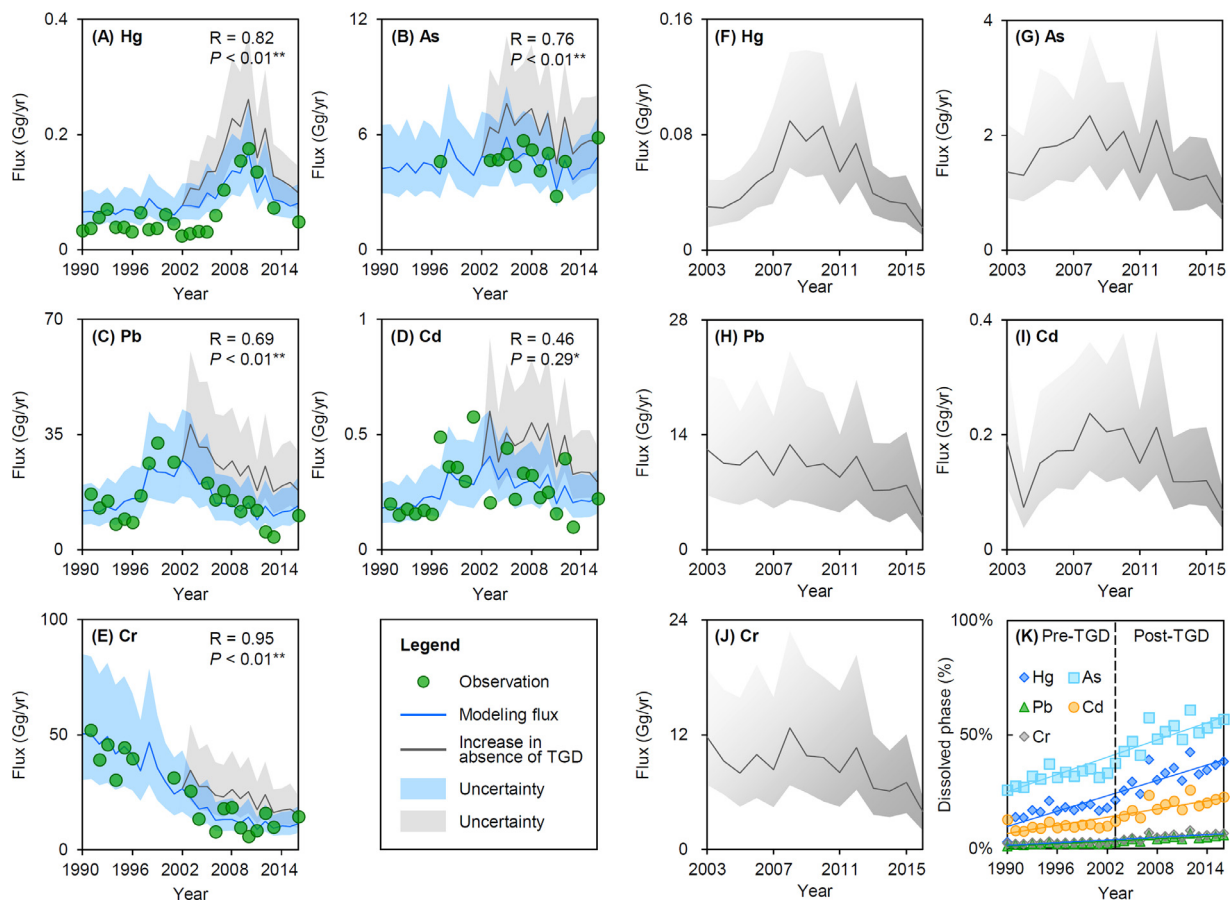


**Fig. 5.** Heavy metal discharges from the Yangtze River into the East China Sea from 1990–2016 and in scenarios of absence of the Three Gorges Dam. Panels (A) to (E) represent Hg, As, Pb, Cd, and Cr discharges from the river, respectively. Panels (F) to (J) represent the amounts of net-accumulations of Hg, As, Pb, Cd, and Cr in the riverbed, respectively. Panel (K) shows the modeling trends of the fractions of dissolved heavy metals to the riverine heavy metal fluxes from 1990–2016. Pre-TGD and Post-TGD represent the periods before and after the construction of the TGD, respectively. Dots in (A) to (E) are observation data and are presented in Table S1, SI. Shaded areas in (A) to (J) represent the P10–90 confidence intervals of the modeling. The line in (K) represents the TGD construction year, 2003.

### 3.3. Impacts of the TGD on heavy metal discharges from the Yangtze River into the East China Sea

We estimated the annual discharge amounts for Hg, As, Pb, Cd, and Cr prior to (1990–2002), and following (2003–2016), the construction of the TGD. A comparison of river metal discharges in 2000 and 2016 showed 28%, 56%, 25%, and 51% decreases for Hg, Pb, Cd, and Cr, respectively, while As discharges remained almost unchanged (Figs. 5A–5E). The construction of the TGD appears to have promoted a net decrease of heavy metal discharge into the sea. This decrease results from the increased sediment deposition upstream of the TGD, especially within the TGR, being greater than the increased erosion of the channel deposits downstream of the TGD (Figs. 2 and 4). The differences in the results for As compared to those of the other metals are mainly a result of the differences in particulate partitioning, as indicated above. In the pre-TGD period (1990–2002), an overwhelming proportion of the heavy metals delivered by the Yangtze River to the East China Sea were particle-bound, representing 83%, 68%, 98%, 90%, and 97% of the Hg, As, Pb, Cd, and Cr fluxes, respectively (Fig. 5K). Owing to TGD-driven perturbations of sediment transport, the particle-associated metal fluxes for Hg, As, Pb, Cd, and Cr decreased to 70%, 48%, 95%, 81%, and 94% in the post-TGD period, i.e., from 2003–2016 (Fig. 5K). The relatively high percentage of Hg present in the dissolved phase (30%) could be related to the 6-fold increase in the concentration of DOC in the downstream waters of the river when compared to the river upstream (Müller et al., 2008), or to analytic

errors in previously published dissolved Hg concentrations (Table S1, SI).

Our results suggest that, in the absence of the TGD, the baseline levels of Cr in the Yangtze River Basin would have decreased from 1990–2016 (Fig. 5E), while the initial decrease of As, Pb, and Cd would have been followed by their increase in 2005, 2002, and 2003, respectively (Figs. 5B–5D). It is thought that the declines in heavy metals loads in Chinese rivers, including the Yangtze River, reflect the implementation of new Chinese environmental policies, which have led to a reduction in the direct anthropogenic release of heavy metals into aquatic environments in recent years, as reported by the government (MEP, 2014). The model-predicted Hg load in the unaltered Yangtze River would have peaked in 2010 (Fig. 5A). This is consistent with its increased usage in industrial applications, such as the production of vinyl chloride monomers, from 2005–2011 and the increase of erosion-induced lateral Hg transport into freshwater ecosystems between the 1990s and early 2010s (Lin et al., 2016; Liu et al., 2018b).

To explore the direct and indirect relationships that could drive heavy metal discharges from the Yangtze River into the East China Sea (Fig. 6), climate-related factors (i.e., precipitation and surface temperature) and human activities (approximated based on the GDP as a predictor of industrial and urban development), together with the influences of the TGD (primarily sediment transport dynamics), were incorporated into a piecewise SEM. The SEM results point to the substantial negative influence of the TGD on sediment discharge into the East China Sea (it contributed a 24% weighted

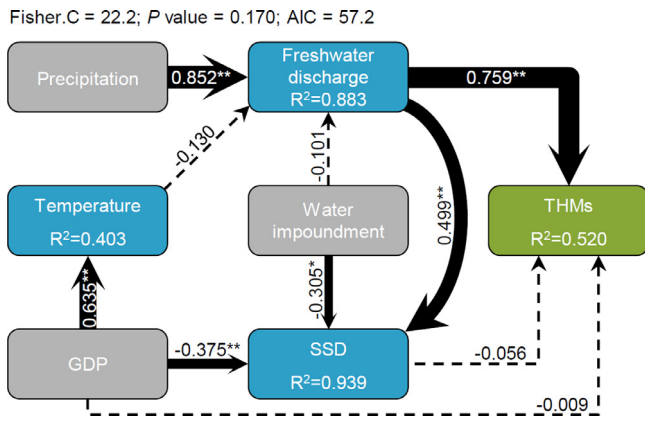


**Fig. 6.** Structural equation model of heavy metal discharges from the Yangtze River into the East China Sea, with climate and human activities as driving factors. Solid arrows represent significant paths ( $P < 0.05$ , piecewise SEM), dotted arrows represent non-significant paths ( $P > 0.05$ , piecewise SEM), and  $R^2$  represents the coefficient of determination. \* $P < 0.05$ , \*\* $P < 0.01$ . Path coefficients are reported as standardized effect sizes. GDP is the gross domestic product, SSD is the suspended sediment discharge, and THM is the total flux of heavy metals into the East China Sea. The standard errors of the standardized coefficients are presented in Fig. S4, SI.

average path coefficient to the discharge variation). This is consistent with the source–sink transport result above. The transport of heavy metals via the Yangtze River is also shown to be influenced by climate-related factors and industrial and urban development (Fig. 6). The positive relationship between freshwater discharge from the river into the East China Sea and precipitation are likely climate driven. A previous study predicted that future seasonal mean precipitation in East Asia would be enhanced by global warming (Qu et al., 2014). Nevertheless, according to the *Bulletin of Ecology and Environment for the Three Gorge Project*, the precipitation in the TGR region has decreased slightly in recent years. Hence, it is too early to conclude that climate change will be an important contributing factor in the overall system, driving heavy metal discharge into the sea (Trenberth, 1998). The positive correlation between GDP and surface temperature indicates that local surface temperature can be significantly influenced by regional development, such as urbanization (Zhou et al., 2004), which has been attributed to the decrease of vegetation coverage and the increase of urban heat island effects (Yao et al., 2017). Elevated surface temperatures may also influence freshwater discharge directly through enhanced evaporation in the Yangtze River Basin (Fig. S3, SI) (Monteith, 1981), but the results of the SEM model suggest that the surface temperature is not a major factor (Fig. 6).

#### 3.4. Fate of heavy metals in the East China Sea and impacts of the TGD

Through the incorporation of these results into a marine mass balance model, we have identified that, despite TGD construction, the Yangtze River was the main terrestrial source of heavy metal (Hg: 58%, As: 73%, Pb: 74%, Cd: 50%, Cr: 74%) in the East China Sea in 2016, while the other terrestrial sources, e.g., other rivers, wastewater, groundwater, soil erosion, and coastal erosion, were less significant (Fig. 7). Previous studies have suggested that Hg discharge from the Yangtze River significantly influences Hg cycling in the coastal seawater and enhances the air–sea exchange of gaseous Hg for the East China Sea (Liu et al., 2019a; Wang et al., 2016). Furthermore, in 2016, the export of Hg and Pb from mainland China was the main source for the East China Sea and accounted for 53% and 71% of total ocean inputs, respectively. However, the majority of these heavy metals that were transported

from the land into the East China Sea were deposited in the sediments of the sea, especially in the estuary and along the shelf, which are characterized by intense flocculation and rapid sedimentation. According to our model, a total of 0.096, 21, 7.6, 0.99, and 24 Gg of Hg, As, Pb, Cd, and Cr were deposited in the estuarine and shelf sediments. The other sources of Hg and Pb were atmospheric deposition, with 14% and 4% contributions, respectively, and ocean currents from the South China and Yellow Seas, which contributed 32% and 25%, respectively. Owing to the relatively recent economic growth and industrialization of China, atmospheric emissions of heavy metals have been increasing in recent years (Cheng et al., 2014), but are still not a substantial source (e.g., As: 0.91%, Cd: 11%, and Cr: 9.3%) for the East China Sea via atmospheric deposition. Mass balance modeling for 2016 revealed that metal transport with ocean currents from adjacent coastal seas accounted for 44%, 65%, 31%, 54%, and 45% of the Hg, As, Pb, Cd, and Cr transported from the East China Sea to the North Pacific Ocean. Furthermore, most of the metals transported to the open ocean originated from the Yellow and South China Seas (Fig. 7), and not from riverine sources. Overall, the North Pacific Ocean is a critical sink for metal contaminants transported into the East China Sea.

Owing to the construction of the TGD, metal burdens in the East China Sea have decreased since the year 2003. According to our model, if the TGD had not been constructed, the estimated masses of metals stored in the water column in 2016 would have been 0.37, 270, 68, 4.8, and 170 Gg of Hg, As, Pb, Cd, and Cr, respectively; 6.9%, 0.99%, 5.1%, 3.8%, and 4.0% higher than that with the TGD (Fig. 8A). These results suggest that, while the operation of the TGD has many impacts on the Yangtze River ecosystem, the largest impact is related to the location of removal of heavy metals, and the relative inputs, via sedimentation, into the East China Sea (Fig. 8D). In 2016, the presence of the TGD decreased fluxes via the sedimentation of particulate heavy metals, by 18%, 1.8%, 34%, 9.0% and 17% for Hg, As, Pb, Cd and Cr, respectively. Transport to other sinks (e.g., removal from the sea by fishing, exports to the North Pacific Ocean, and evasion from the sea surface) decreased by between 1.1% and 9.8% in 2013 (Figs. 8B, 8C, and 8E). We conclude that, currently, the presence of the TGD has decreased the heavy metal burden of the East China Sea. However, a previous study forecasted that the current net accumulation of suspended sediment in the Yangtze River will switch to net depletion from 2030–2100, because: (1) the suspended sediment concentrations in the upstream freshwater discharge will continue to decrease owing to forest protection programs; and (2) there is a plethora of erodible depositions (approximately 100,000 Tg of sediment) along the mid-lower stretches of the river, deposited since the Holocene (Yang et al., 2014). With such a large amount of erodible sediment, the legacy heavy metals accumulated in the river section downstream of the TGD might have a persistent impact on the ecology of the river and sea.

#### 3.5. Uncertainty analysis

The uncertainties of the heavy metal estimates directly exported from rivers, wastewater, groundwater, soil erosion, and coastal erosion into the East China Sea are also provided in Fig. S7, SI. The uncertainties of the heavy metal discharges from the Yangtze River were -31% to 49% (P10–90 confidence interval), -31% to 45%, -32 to 47%, -32% to 50%, and -33% to 52% for Hg, As, Pb, Cd, and Cr, respectively, in 2016 (Figs. 5A to 5E). Most of the results fall within acceptable ranges, compared with previous studies (Cheng et al., 2014; Wang et al., 2012). It should be noted that the uncertainties for some sectors seem to be large. Some previous studies have used 50% or 60% of the confidence interval to represent the uncertainty (Wang et al., 2012; Wu et al., 2012). In this study, 80% of the confidence interval was selected to clearly repre-

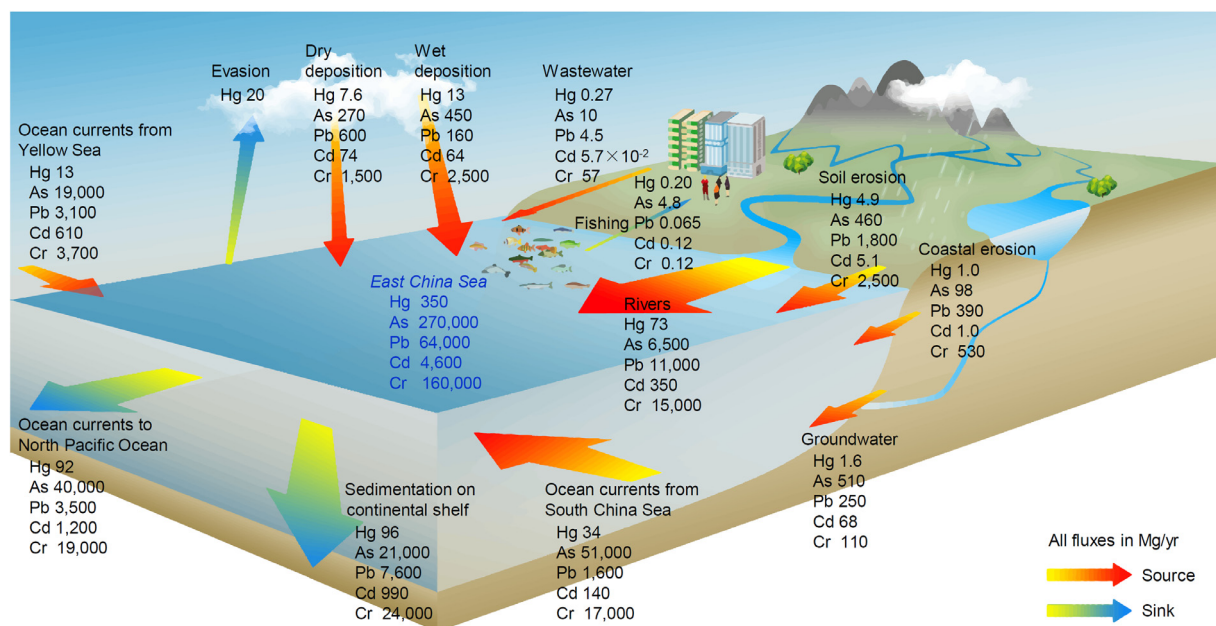


Fig. 7. Mass balances of heavy metals in the East China Sea in 2016. Source, flux of heavy metals into the seawater; sink, loss of heavy metals from the seawater.

sent the distribution of results (Wu et al., 2010). The overall uncertainties of the mass balance model are summarized based on the model results of the heavy metal concentrations in the seawater of the East China Sea (Fig. 8F). The uncertainties of the mass balance models were estimated to be -42% to 44%, -63% to 71%, -36% to 68%, -45% to 47%, and -53% to 56% for the concentrations of Hg, As, Pb, Cd, and Cr, respectively, in 2013. Overall, the observational data from previous studies and the results of the mass balance models are comparable (Fig. 8F). The overall uncertainties of the mass balance models are not insignificant, especially for the estimates of the amounts of heavy metal being exchanged by ocean currents, and they range from -130% to 230%, primarily owing to a lack of data. Additionally, the analytical errors associated with the heavy metal concentration measurements in the published literature and the present study, as well as errors in the data used for the riverine freshwater and suspended sediment discharge inventories in this study, contribute to the uncertainty of the modeling results. However, despite these uncertainties, the similarity between the observations and the modeled riverine metal fluxes (Figs. 5A–5E), as well as the model estimates of oceanic heavy metal concentrations (Fig. 8F), indicate that the model results are reasonable. Based on sedimentary records, previous studies found that sedimentary ratios of Hg and Pb in the East China Sea peaked in the early 2000s, while that for As changed little before the 2000s but also increased slightly in the last decade (Chen et al., 2014; Dong et al., 2012; Duan et al., 2015; Zhang et al., 2018); this similar to our estimates (Figs. 5A–5E). Nevertheless, the sedimentary records of heavy metals in the results of different studies vary widely, probably owing to the heterogeneity of sediment distributions. Therefore, these results need further verification.

### 3.6. Implications for future study

This study is the first attempt to quantitatively evaluate the impact that a large dam, such as the TGD, has on heavy metal fluxes across the river–ocean continuum. Operation of the TGD could substantially decrease fluvial fluxes of heavy metals by impounding them within the dam reservoir, i.e., the TGR, and in other segments of the river that are located upstream of the dam. In contrast, heavy metal fluxes into the coastal ocean could be increased

through the downstream depletion of legacy metals from riverbed and bank erosion. Therefore, a decreased flux of heavy metals upstream and their increase downstream could occur simultaneously, with a variable net impact on the fluxes of different constituents into the East China Sea over time. In many cases, materials trapped in reservoirs have been investigated, albeit omitting the significance of reservoir construction on sediment erosion downstream of the dam (Yang et al., 2014). Our analysis provides additional evidence that large dams substantially alter contaminant fluxes throughout the river, and not just above the reservoir. Our evaluation, using a combination of previous studies, our own measurements, and model analyses, shows that the impacts of large dams, such as the TGD, can have a long spatial range, e.g., ~2,000 km in the case of the TGD (Yang et al., 2014). Moreover, heavy metals bound to suspended sediment transported by the Yangtze River into the sea can be further transported hundreds of kilometers offshore via ocean currents.

Although our results provide different predictions for the various metals examined, we acknowledge that it is challenging to describe exactly how large dams influence the fluxes of metal contaminants, and there are several caveats and limitations to our study. In addressing these limitations, we included the calculation of uncertainties and details of such uncertainty analyses in this paper. In this study, the samples were mainly collected in one year. Although more time-series observational data are needed, collections are labor-intensive and costly. We have therefore relied on heavy metal fluxes calculated from the available data, based on the relatively constant conditions in recent years, in terms of freshwater discharge and suspended sediment. We have considered seasonal changes in the heavy metal concentrations in the water column at each sampling site and incorporated this into our estimates. Our research relied on subsurface water sampling, given the difficulty of sampling at many locations where there were extremely strong currents. Other studies have also relied on subsurface water samples (Buck et al., 2015; Emmerton et al., 2013; Müller et al., 2008).

Notably, our modeling of heavy metal discharges from the Yangtze River in the absence of the TGD is subject to large uncertainty, since we were unable to consider biogeochemical changes in the heavy metals in the no-TGD scenario. The inclusion of bio-

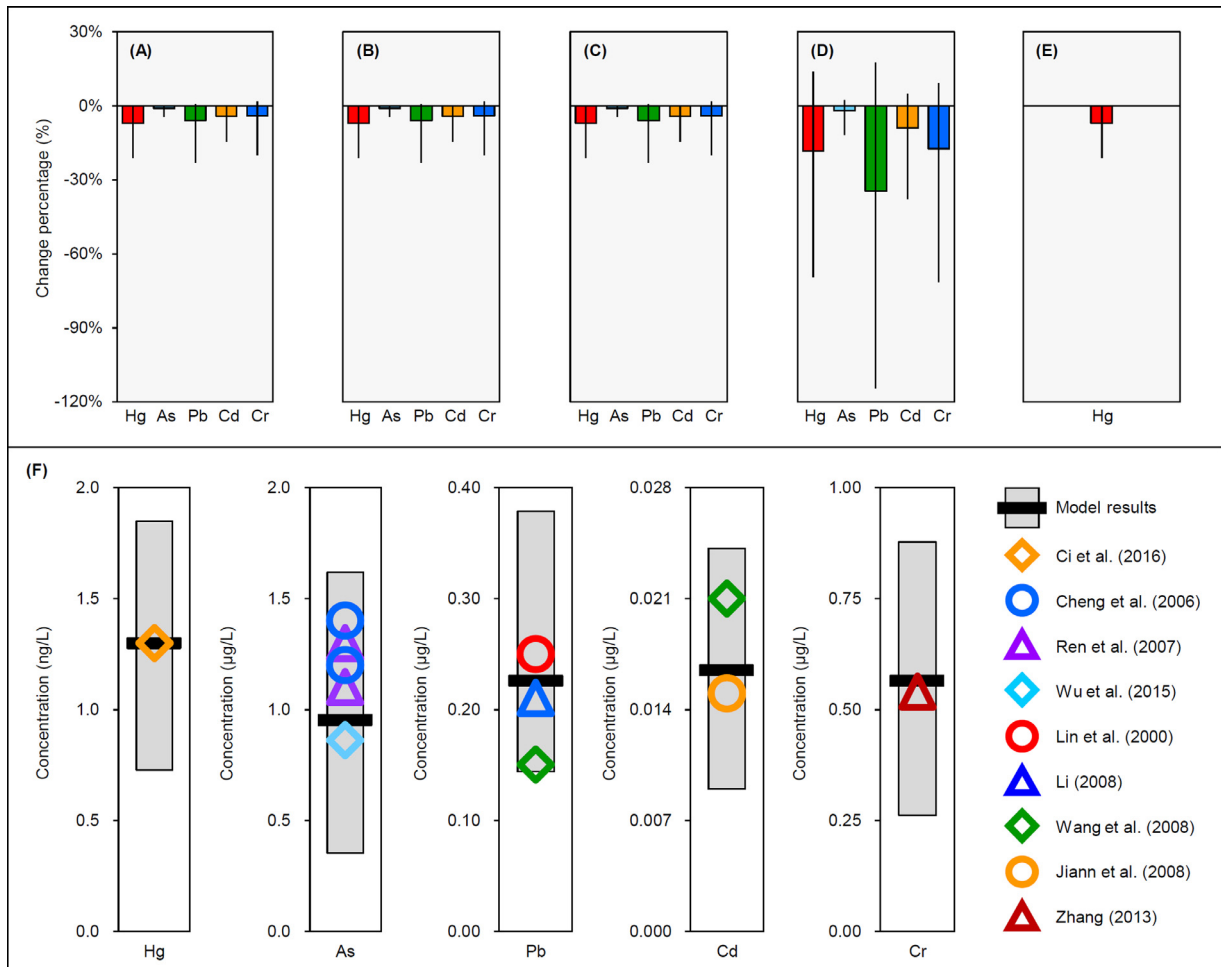


**Fig. 8.** Changes to heavy metal concentrations and sinks in the East China Sea owing to the Three Gorges Dam in 2016 ((A) to (E)) and the uncertainties of the heavy metal concentrations in the model (F). Panel (A): changes of heavy metal concentrations in the East China Sea. Panel (B): heavy metal removal from the sea by fishing. Panel (C): export of heavy metals by ocean currents to the North Pacific Ocean. Panel (D): removal of heavy metals by sedimentation onto the seabed. Panel (E): Hg evasion from the sea surface. In Panels (A) to (E), bars indicate the P10–90 confidence intervals given by the uncertainty analysis. In panel (F), the thick black horizontal lines are the modeled concentrations, and the gray bars are the uncertainties of the concentrations of heavy metals in the East China Sea in 2013 (P10–90 confidence intervals). Other symbols (diamonds, circles, and triangles) in panel (F) are the observational data of heavy metals in the East China Sea from previous studies (Cheng et al., 2006; Ci et al., 2016; Jiann et al., 2009; Li, 2008; Lin et al., 2000; Ren et al., 2007; Wang et al., 2010; Wu et al., 2015; Zhang, 2013).

geochemical processes was outside the scope of this study and additional research is required to study the biogeochemical transformation of metals in the water and their interactions with particles along the river and within the estuary. Another level of uncertainty is related to analytical errors in the previously published heavy metal concentrations. Hence, our estimates of the heavy metal fluxes along the Yangtze River and into the sea should be further updated. Additionally, the river–ocean continuum (i.e., river–estuary–shelf–open ocean) is a complex and rapidly changing system, owing to both natural and human-driven impacts. For instance, our model cannot account for differences in the extent of flocculation owing to the lack of field data, which is a motivation for such studies in the future.

This study aimed to shed light on the potential influence that large dams have on contaminant cycling in the environment. As noted earlier, approximately 50,000 large dams are operating worldwide (Lempérière, 2006); therefore, the case made by the present study is of relevance to many other areas where rivers are obstructed by large dams. River damming is increasing in the river basins of Asia, South America, and Africa, and the Amazon, Yangtze, and Ganges Basins may become primary hotspots for pollution accumulation and depletion in the world (Latrubesse et al., 2017; Maavara et al., 2017). Further research should be conducted

on these river basins and their adjacent seas, to examine the substantial impacts caused by large dams on contaminant biogeochemical cycles.

#### 4. Conclusions

In this study, we found that the TGD can significantly impact metal contaminant transport in the Yangtze River–East China Sea continuum. The Yangtze River discharges substantial amounts of heavy metals into the coastal ocean, and the wet seasons are responsible for a large proportion of the annual heavy metal fluxes. Although substantial amounts of these metals were impounded in the TGR and only a relatively small fraction was discharged into the Yangtze River downstream of the reservoir, the operation of the TGD induced remarkable resuspension of these metals in the downstream section of the river and their delivery into the coastal ocean. Metal flux alteration was primarily attributed to the altered hydrology caused by the operation of the TGD. Therefore, metal fluxes to the coastal ocean were primarily derived from the downstream portion of the river, while the contributions of additional sources were relatively small. Currently, the presence of the TGD decreases the heavy metal burdens on the East China Sea. However, this may change in future because there is a plethora

of erodible deposition along the mid-lower stretches of the river that have been deposited since the Holocene. Overall, we conclude that the world's largest hydropower construction, the TGD, has had a significant impact on pollutant transport throughout the Yangtze River and into the East China Sea. The results of our research should be considered in other geographic locations where large dams are constructed on large rivers.

### Supporting Information

The Supporting Information includes a photo of the TGD (Fig. S1); the major rivers around the East China Sea (Fig. S2); a scatter-plot matrix of the relationships of different variables with the flux of heavy metals (Fig. S3); uncertainty in the SEM (Fig. S4); riverine discharge of heavy metals into the East China Sea (Fig. S5); relationships between TSS and heavy metal concentrations (Fig. S6); uncertainties in the fate of heavy metals in the East China Sea (Fig. S7); heavy metal concentrations in riverine water (Table S1), groundwater (Table S2) and coastal soil (Table S3); the erosion rates (Table S4) and erosion modulus (Table S5) of coastal soil; the parameters of the marine mass balance models (Table S6); a comparison of heavy metal fluxes in the published literature (Table S7); and the heavy metal concentration results fitted to the TSS (Table S8).

### Declaration of Competing Interest

The authors declare that they have no known competing financial interests or personal relationships that could have appeared to influence the work reported in this paper.

### Acknowledgments

We would like to thank the editor and the anonymous reviewers for their invaluable comments. This work was funded by the National Natural Science Foundation of China (No. 41977311, 41977324, 41630748, and 41821005). The involvement of Robert P. Mason was supported by the Dartmouth National Institute of Health Superfund Program grant (No. P42 ES007373).

### Supplementary materials

Supplementary material associated with this article can be found, in the online version, at doi:10.1016/j.watres.2020.116295.

### References

Amos, H.M., Jacob, D.J., Kocman, D., Horowitz, H.M., Zhang, Y., Dutkiewicz, S., Horvat, M., Corbitt, E.S., Krabbenhoft, D.P., Sunderland, E.M., 2014. Global biogeochemical implications of mercury discharges from rivers and sediment burial. *Environ. Sci. Technol.* 48 (16), 9514–9522.

An, Q., Wu, Y., Wang, J., Li, Z., 2010. Assessment of dissolved heavy metal in the Yangtze River estuary and its adjacent sea. *China. Environ. Monit. Assess* 164 (1–4), 173–187.

Bond, T.C., Bhardwaj, E., Dong, R., Jogani, R., Jung, S., Roden, C., Streets, D.G., Trautmann, N.M., 2007. Historical emissions of black and organic carbon aerosol from energy-related combustion, 1850–2000. *Glob. Biogeochem. Cycle* 21 (2), 1–16.

Brandt, S.A., 2000. Classification of geomorphological effects downstream of dams. *Catena* 40 (4), 375–401.

Buck, C.S., Hammerschmidt, C.R., Bowman, K.L., Gill, G.A., Landing, W.M., 2015. Flux of total mercury and methylmercury to the northern Gulf of Mexico from US estuaries. *Environ. Sci. Technol.* 49 (24), 13992–13999.

Chen, B., Fan, D., Li, W., Wang, L., Zhang, X., Liu, M., Guo, Z., 2014. Enrichment of heavy metals in the inner shelf mud of the East China Sea and its indication to human activity. *Cont. Shelf Res.* 90, 163–169.

Chen, K., Liu, X., Ding, L., Huang, G., Li, Z., 2016. Spatial characteristics and driving factors of provincial wastewater discharge in China. *Int. J. Environ. Res. Public Health* 13 (12), 1221–1240.

Cheng, K., Wang, Y., Tian, H., Gao, X., Zhang, Y., Wu, X., Zhu, C., Gao, J., 2014. Atmospheric Emission Characteristics and Control Policies of Five Precedent-Controlled Toxic Heavy Metals from Anthropogenic Sources in China. *Environ. Sci. Technol.* 49 (2), 1206–1214.

Cheng, S., 2003. Heavy metal pollution in China: origin, pattern and control. *Environ. Sci. Pollut. Res.* 10 (3), 192–198.

Cheng, Y., Ren, J., Li, D., Liu, S., Zhang, J., 2006. Distribution of dissolved inorganic arsenic and its seasonal variations in the coastal area of the east China sea. *J. Ocean Univ. China* 5 (3), 243–250.

Ci, Z., Zhang, X., Yin, Y., Chen, J., Wang, S., 2016. Mercury Redox Chemistry in Waters of the Eastern Asian Seas: From Polluted Coast to Clean Open Ocean. *Environ. Sci. Technol.* 50 (5), 2371–2380.

Dai, A.G., Qian, T.T., Trenberth, K.E., Milliman, J.D., 2008. Changes in Continental Freshwater Discharge from 1948 to 2004. *J. Clim.* 22 (10), 2773–2792.

Dong, A., Zhai, S., Zabel, M., Yu, Z., Zhang, H., Liu, F., 2012. Heavy metals in Changjiang estuarine and offshore sediments: responding to human activities. *Acta Oceanol. Sin.* 31 (2), 88–101.

Duan, L.-Q., Song, J.-M., Yu, Y., Yuan, H.-M., Li, X.-G., Li, N., 2015. Spatial variation, fractionation and sedimentary records of mercury in the East China Sea. *Mar. Pollut. Bull.* 101 (1), 434–441.

Duruibe, J.O., Ogwuegbu, M., Ekwurugwu, J., 2007. Heavy metal pollution and human biotoxic effects. *Int. J. Phys. Sci.* 2 (5), 112–118.

Emmerton, C.A., Graydon, J.A., Gareis, J.A., St. Louis, V.L., Lesack, L.F., Banack, J.K., Hicks, F., Nafziger, J., 2013. Mercury export to the Arctic Ocean from the Mackenzie River, Canada. *Environ. Sci. Technol.* 47 (14), 7644–7654.

Gao, L., Gao, B., Xu, D., Peng, W., Lu, J., 2019. Multiple assessments of trace metals in sediments and their response to the water level fluctuation in the Three Gorges Reservoir, China. *Sci. Total Environ.* 648, 197–205.

Grübler, A., Nakićenović, N., Victor, D.G., 1999. Dynamics of energy technologies and global change. *Energy policy* 27 (5), 247–280.

Hammerschmidt, C.R., Fitzgerald, W.F., Lamborg, C.H., Balcom, P.H., Tseng, C.-M., 2006. Biogeochemical cycling of methylmercury in lakes and tundra watersheds of Arctic Alaska. *Environ. Sci. Technol.* 40 (4), 1204–1211.

Humborg, C., Ittekkot, V., Cociasu, A., Bodungen, B.V., 1997. Effect of Danube River dam on Black Sea biogeochemistry and ecosystem structure. *Nature* 386 (6623), 385–388.

Ittekkot, V., Humborg, C., Schäfer, P., 2000. Hydrological Alterations and Marine Biogeochemistry: A Silicate Issue? Silicate retention in reservoirs behind dams affects ecosystem structure in coastal seas. *AIBS Bull.* 50 (9), 776–782.

Järup, L., 2003. Hazards of heavy metal contamination. *Br. Med. Bull.* 68 (1), 167–182.

Jiann, K.-T., Wen, L.-S., Gong, G.-C., 2009. Distribution and behaviors of Cd, Cu, and Ni in the East China sea surface water off the Changjiang Estuary. *Terr. Atmos. Ocean. Sci.* 20 (2), 433–443.

Latrubesse, E.M., Arima, E.Y., Dunne, T., Park, E., Baker, V.R., d'Horta, F.M., Wight, C., Wittmann, F., Zuanon, J., Baker, P.A., 2017. Damming the rivers of the Amazon basin. *Nature* 546 (7658), 363–369.

Lawson, N.M., Mason, R.P., Laporte, J.-M., 2001. The fate and transport of mercury, methylmercury, and other trace metals in Chesapeake Bay tributaries. *Water Res.* 35 (2), 501–515.

Lefcheck, J.S., 2016. piecewiseSEM: Piecewise structural equation modelling in R for ecology, evolution, and systematics. *Methods Ecol. Evol.* 7 (5), 573–579.

Lempérière, F., 2006. The role of dams in the XXI century. *Int. J. hydropower dams* 3, 99–109.

Li, L. (2008) The distribution of dissolved heavy metals in the southern Yellow Sea, Master's Thesis, the First Institute of Oceanography, SOA.

Lin, F., Hsu, S.C., Jeng, W.L., 2000. Lead in the southern East China Sea. *Mar. Environ. Res.* 49 (4), 329–342.

Lin, Y., Wang, S., Wu, Q., Larssen, T., 2016. Material flow for the intentional use of mercury in China. *Environ. Sci. Technol.* 50 (5), 2337–2344.

Liu, C., Chen, L., Liang, S., Li, Y., 2019a. Distribution of total mercury and methylmercury and their controlling factors in the East China Sea. *Environ. Pollut.* 258. doi:10.1016/j.envpol.2019.113667.

Liu, M., Chen, L., Wang, X., Zhang, W., Tong, Y., Ou, L., Xie, H., Shen, H., Ye, X., Deng, C., Wang, H., 2016a. Mercury Export from Mainland China to Adjacent Seas and Its Influence on the Marine Mercury Balance. *Environ. Sci. Technol.* 50 (12), 6224–6232.

Liu, M., Du, P., Yu, C., He, Y., Zhang, H., Sun, X., Lin, H., Luo, Y., Xie, H., Guo, J., Li, X., Wang, X., 2017. Increases of Total Mercury and Methylmercury Releases from Municipal Sewage into Environment in China and Implications. *Environ. Sci. Technol.* 52 (1), 124–134.

Liu, M., He, Y., Baumann, Z., Yu, C., Ge, S., Sun, X., Cheng, M., Shen, H., Mason, R.P., Chen, L., Zhang, Q., Wang, X., 2018a. Traditional Tibetan Medicine Induced High Methylmercury Exposure Level and Environmental Mercury Burden in Tibet, China. *Environ. Sci. Technol.* 52 (15), 8838–8847.

Liu, M., Xie, H., He, Y., Zhang, Q., Sun, X., Yu, C., Chen, L., Zhang, W., Zhang, Q., Wang, X., 2019b. Sources and transport of methylmercury in the Yangtze River and the impact of the Three Gorges Dam. *Water Res.* 166 (1). doi:10.1016/j.watres.2019.115042.

Liu, M., Zhang, Q., Ge, S., Mason, R.P., Luo, Y., He, Y., Xie, H., Sa, R., Chen, L., Wang, X., 2019c. Rapid Increase in the Lateral Transport of Trace Elements Induced by Soil Erosion in Major Karst Regions in China. *Environ. Sci. Technol.* 53 (8), 4206–4214.

Liu, M., Zhang, Q., Luo, Y., Mason, R.P., Ge, S., He, Y., Yu, C., Sa, R., Cao, H., Wang, X., 2018b. Impact of Water-induced Soil Erosion on the Terrestrial Transport and Atmospheric Emission of Mercury in China. *Environ. Sci. Technol.* 52 (12), 6945–6956.

Liu, M., Zhang, W., Wang, X., Chen, L., Wang, H., Luo, Y., Zhang, H., Shen, H., Tong, Y., Ou, L., 2016b. Mercury Release to Aquatic Environments from Anthropogenic Sources in China from 2001 to 2012. *Environ. Sci. Technol.* 50 (15), 8169–8177.

- Maavara, T., Lauerwald, R., Regnier, P., Van Cappellen, P., 2017. Global perturbation of organic carbon cycling by river damming. *Nat. Commun.* 8, 15347–15356.
- Maavara, T., Parsons, C.T., Ridenour, C., Stojanovic, S., Dürr, H.H., Powley, H.R., Van Cappellen, P., 2015. Global phosphorus retention by river damming. *Proc. Natl. Acad. Sci. U. S. A* 112 (51), 15603–15608.
- Matschullat, J., 2000. Arsenic in the geosphere – a review. *Sci. Total Environ.* 249 (1–3), 297–312.
- Mayor, J.R., Sanders, N.J., Classen, A.T., Bardgett, R.D., Clément, J.C., Fajardo, A., Lavorel, S., Sundqvist, M.K., Bahn, M., Chisholm, C., 2017. Elevation alters ecosystem properties across temperate treelines globally. *Nature* 542 (7639), 91–95.
- MEP, 2014. China Environmental Statistics Yearbook. Ministry of Environmental Protection (MEP), Beijing: China.
- Monteith, J.L., 1981. Evaporation and surface temperature. *Q. J. R. Meteorol. Soc.* 107 (451), 1–27.
- Müller, B., Berg, M., Yao, Z., Zhang, X., Wang, D., Pflüger, A., 2008. How polluted is the Yangtze river? Water quality downstream from the Three Gorges Dam. *Sci. Total Environ.* 402 (2), 232–247.
- MWR, 2016 a. China River Sediment Bulletin. Ministry of Water Resources (MWR), Beijing: China.
- MWR, 2016 b. Hydrologic Data Yearbook. Ministry of Water Resources (MWR), Beijing: China.
- NBS, 2014. China Statistical Yearbook. National Statistics Bureau (NBS), Beijing: China.
- Nriagu, J.O., 1989. A global assessment of natural sources of atmospheric trace metals. *Nature* 338 (6210), 47–49.
- Nriagu, J.O., Pacyna, J.M., 1988. Quantitative assessment of worldwide contamination of air, water and soils by trace metals. *Nature* 333 (6169), 134–139.
- Outridge, P.M., Mason, R.P., Wang, F., Guerrero, S., Heimbürger-Boavida, L., 2018. Updated global and oceanic mercury budgets for the United Nations Global Mercury Assessment 2018. *Environ. Sci. Technol.* 52 (20), 11466–11477.
- Pacyna, E.G., Pacyna, J.M., Steenhuisen, F., Wilson, S., 2006. Global anthropogenic mercury emission inventory for 2000. *Atmos. Environ.* 40 (22), 4048–4063.
- Pirrone, N., Cinnirella, S., Feng, X., Finkelman, R.B., Friedli, H.R., Leaner, J., Mason, R., Mukherjee, A.B., Stracher, G.B., Streets, D., 2010. Global mercury emissions to the atmosphere from anthropogenic and natural sources. *Atmos. Chem. Phys.* 10 (13), 5951–5964.
- Poff, N.L., Olden, J.D., Merritt, D.M., Pepin, D.M., 2007. Homogenization of regional river dynamics by dams and global biodiversity implications. *Proc. Natl. Acad. Sci. U. S. A* 104 (14), 5732–5737.
- Qu, X., Huang, G., Zhou, W., 2014. Consistent responses of East Asian summer mean rainfall to global warming in CMIP5 simulations. *Theor. Appl. Climatol.* 117 (1–2), 123–131.
- Raschid-Sally, L. and Jayakody, P. (2009) Drivers and characteristics of wastewater agriculture in developing countries: Results from a global assessment, International Water Management Institute, Colombo, Sri Lanka.
- Raymond, P.A., Saiers, J.E., Sobczak, W.V., 2016. Hydrological and biogeochemical controls on watershed dissolved organic matter transport: Pulse-shunt concept. *Ecology* 97 (1), 5–16.
- Regnier, P., Friedlingstein, P., Ciais, P., Mackenzie, F.T., Gruber, N., Janssens, I.A., Laruelle, G.G., Lauerwald, R., Luysaert, S., Andersson, A.J., 2013. Anthropogenic perturbation of the carbon fluxes from land to ocean. *Nat. Geosci.* 6 (8), 597–607.
- Ren, J., Li, D., Zhang, J., Liu, S., Lv, R., 2007. Species and distribution of dissolved inorganic arsenic in the Yellow Sea and East China Sea. *Mar. Environ. Sci.* 26 (3), 211–216.
- Schartup, A.T., Balcom, P.H., Soerensen, A.L., Gosnell, K.J., Calder, R.S., Mason, R.P., Sunderland, E.M., 2015. Freshwater discharges drive high levels of methylmercury in Arctic marine biota. *Proc. Natl. Acad. Sci. U. S. A* 112 (38), 11789–11794.
- Shipley, B., 2013. The AIC model selection method applied to path analytic models compared using ad-separation test. *Ecology* 94 (3), 560–564.
- Sonke, J.E., Teisserenc, R., Heimbürger-Boavida, L.-E., Petrova, M.V., Maruscak, N., Le Dantec, T., Chupakov, A.V., Li, C., Thackray, C.P., Sunderland, E.M., 2018. Eurasian river spring flood observations support net Arctic Ocean mercury export to the atmosphere and Atlantic Ocean. *Proc. Natl. Acad. Sci. U. S. A* 115 (50), E11586–E11594.
- Stone, R., 2008. Three Gorges Dam: Into the Unknown. *Science* 321 (5889), 628–632.
- Streets, D.G., Bond, T.C., Lee, T., Jang, C., 2004. On the future of carbonaceous aerosol emissions. *J. Geophys. Res.-Atmos.* 109 (D24), 1–19.
- Streets, D.G., Devane, M.K., Lu, Z., Bond, T.C., Sunderland, E.M., Jacob, D.J., 2011. All-time releases of mercury to the atmosphere from human activities. *Environ. Sci. Technol.* 45 (24), 10485–10491.
- Syvitski, J.P., Vörösmarty, C.J., Kettner, A.J., Green, P., 2005. Impact of humans on the flux of terrestrial sediment to the global coastal ocean. *Science* 308 (5720), 376–380.
- Trenberth, K.E., 1998. Atmospheric moisture residence times and cycling: Implications for rainfall rates and climate change. *Clim. Change* 39 (4), 667–694.
- Volesky, B., Holan, Z.R., 1995. Biosorption of heavy metals. *Biotechnol. Prog.* 11 (3), 235–250.
- Vukovic, D., Vukovic, Z., Stankovic, S., 2014. The impact of the Danube Iron Gate Dam on heavy metal storage and sediment flux within the reservoir. *Catena* 113, 18–23.
- Wai, K.-M., Wu, S., Li, X., Jaffe, D.A., Perry, K.D., 2016. Global atmospheric transport and source-receptor relationships for arsenic. *Environ. Sci. Technol.* 50 (7), 3714–3720.
- Wang, C., Ci, Z., Wang, Z., Zhang, X., 2016. Air-sea exchange of gaseous mercury in the East China Sea. *Environ. Pollut.* 212, 535–543.
- Wang, C., Wang, X., Li, K., Liang, S., Su, R., Yang, S., 2010. The estimation of copper, lead, zinc and cadmium fluxes into the sea area of the East China Sea interfered by terrigenous matter and their environmental capacities. *Acta Oceanol. Sin.* 32 (4), 62–76 in Chinese.
- Wang, R., Tao, S., Wang, W., Liu, J., Shen, H., Shen, G., Wang, B., Liu, X., Li, W., Huang, Y., 2012. Black carbon emissions in China from 1949 to 2050. *Environ. Sci. Technol.* 46 (14), 7595–7603.
- Wu, B., Song, J., Li, X., 2015. Distribution and chemical speciation of dissolved inorganic arsenic in the Yellow Sea and East China Sea. *Acta Oceanol. Sin.* 34 (6), 12–20.
- Wu, J., Huang, J., Han, X., Xie, Z., Gao, X., 2003. Three-Gorges Dam–experiment in habitat fragmentation? *Science* 300 (5623), 1239–1240.
- Wu, Q., Wang, S., Zhang, L., Song, J., Yang, H., Meng, Y., 2012. Update of mercury emissions from China's primary zinc, lead and copper smelters, 2000–2010. *Atmos. Chem. Phys.* 12 (22), 11153–11163.
- Wu, Y., Streets, D.G., Wang, S., Hao, J., 2010. Uncertainties in estimating mercury emissions from coal-fired power plants in China. *Atmos. Chem. Phys.* 10 (6), 2937–2946.
- Yang, S., Milliman, J., Xu, K., Deng, B., Zhang, X., Luo, X., 2014. Downstream sedimentary and geomorphic impacts of the Three Gorges Dam on the Yangtze River. *Earth-Sci. Rev.* 138, 469–486.
- Yang, S., Zhao, Q., Belkin, I.M., 2002. Temporal variation in the sediment load of the Yangtze river and the influences of human activities. *J. Hydrol.* 263 (s 1–4), 56–71.
- Yao, R., Wang, L., Gui, X., Zheng, Y., Zhang, H., Huang, X., 2017. Urbanization Effects on Vegetation and Surface Urban Heat Islands in China's Yangtze River Basin. *Remote Sens* 9 (6), 540–556.
- Zhang, R., Russell, J., Xiao, X., Zhang, F., Li, T., Liu, Z., Guan, M., Han, Q., Shen, L., Shu, Y., 2018. Historical records, distributions and sources of mercury and zinc in sediments of East China sea: Implication from stable isotopic compositions. *Chemosphere* 205, 698–708.
- Zhang, Y. (2013) Heavy metal process in water and pollution risk assessment in surface sediments of the Yellow River Estuary, Yangtze Estuary and Pearl River Estuary, Master's Thesis, Third Institute of Oceanography, State Oceanic Administration.
- Zhao, J., Jiang, Y., Yan, B., Wei, C., Zhang, L., Ying, G., 2014. Multispecies acute toxicity evaluation of wastewaters from different treatment stages in a coking wastewater-treatment plant. *Environ. Toxicol. Chem.* 33 (9), 1967–1975.
- Zhou, L., Dickinson, R.E., Tian, Y., Fang, J., Li, Q., Kaufmann, R.K., Tucker, C.J., Myrneni, R.B., 2004. Evidence for a significant urbanization effect on climate in China. *Proc. Natl. Acad. Sci. U. S. A* 101 (26), 9540–9544.
- Zhu, H., Bing, H., Wu, Y., Zhou, J., Sun, H., Wang, J., Wang, X., 2019. The spatial and vertical distribution of heavy metal contamination in sediments of the Three Gorges Reservoir determined by anti-seasonal flow regulation. *Sci. Total Environ.* 664, 79–88.